Estimates of Downward Surface Radiation over China

Jianqing XU (FRSGC), Tadahiro HAYASAKA,
Kazuaki KAWAMOTO (RIHN), and Shigenori HAGINOYA (MRI)

1. Introduction

Jordan sunshine recorder is a kind of direct solar radiation recorder (**Fig.1**). Sunlight penetrates a small hole on the side of a copper cylinder, hitting light-sensitive paper inside. The paper is changed daily. The length of the burned line on the light-sensitive paper is a measure of the sunshine duration. This is a very simple observation method that needs no electricity and is easily maintained. However, the recorder may omit time when the sun is at low altitudes (about 5°in city and 2°in rural area). Solar radiation data have been recorded for more than 50 years over most areas of China. Downward surface solar and long-wave radiation fluxes can be derived from sunshine duration data using parameters from a Jordan sunshine recorder. In the past 20 years, satellite observations and routine surface meteorological observations have occurred simultaneously. Two principal factors drive the development of this method. Although satellite data can be used effectively to analyze the surface radiation budget, the time period covered by the satellite-based SRB dataset (NASA Langley Research Center) is insufficient for climatic analysis.

2. Calculation method

Routine meteorological datasets were used to estimate downward surface solar and long-wave radiation fluxes. Downward surface solar radiation flux was derived from sunshine duration data using parameters from a Jordan sunshine recorder. Downward surface long-wave radiation flux was estimated from the surface air humidity, temperature, and calculated downward surface solar radiation. The influence of topography or high altitude was also considered. Calculations were checked against in situ observations.

Fig. 2; Revising raw sunshine duration data. Solid lines are the seasonal changes of different solar altitudes (2°, 4°, …20°). Upper panel is Jiuquan (39°46'N, 98°29'E, 1477m asl), lower panel is Baingoin (31°22'N, 90°01'E, 4700m asl). Marks are Nobs/N0 on fine days. If a meteorological station is in a valley or surrounded by high buildings, the observed sunshine duration can be shorter than its true value. Observed raw data should be revised for such cases. At Jiuquan, the ratios of Nobs/N0 exceed 0.92 and the

marks can be put around 2°- 4°of the solar altitude: the meteorological observatory at Jiuquan is in a open area without nearby mountains or buildings, so N=NObs there.

Fig. 1. The Jordan sunshine recorder.

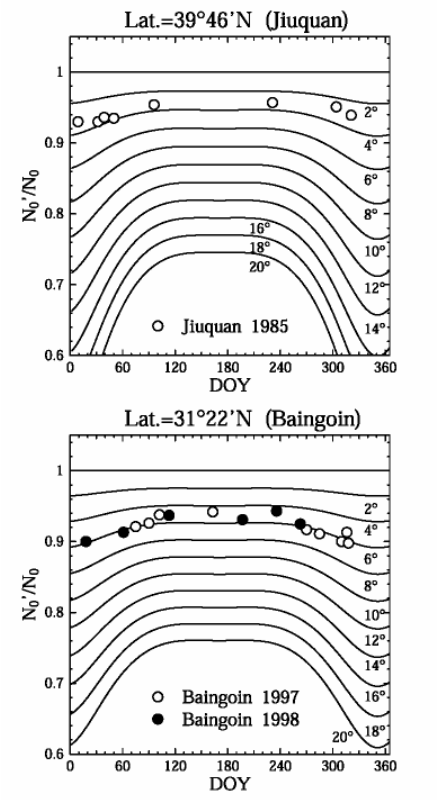

Fig. 2

Fig. 3; Seasonal changes in the ratios of sunshine duration Nobs/N0. Top panel is from the observed raw data, middle panel the revised data, and bottom panel the precipitation at Baingoin in 1998. At Baingoin, Nobs/N0 is sometimes less than 0.9, and the marks are placed between 4°- 7°. Sunlight is blocked when the solar altitude is less than about 5°. Baingoin may be in a valley on the Tibetan Plateau, and N≠NObs there.

Fig. 4; Seasonal changes in calculated solar radiation fluxes at Jiuquan in 1985. The solid line is the daily downward solar radiation SM↓, as estimated from sunshine duration. The dotted line is the daily downward solar radiation under clear sky conditions SMf↓ whenβDUST = 0.1. The broken line is SMf↓ when βDUST = 0.03. The dashed line is SMf↓ when βDUST = 0.0. WhenβDUST = 0.03, SMf↓adjusts SM↓ well. In winter, βDUST may be less than 0.03. In the present study, βDUST is assumed constant, with no seasonal changes.

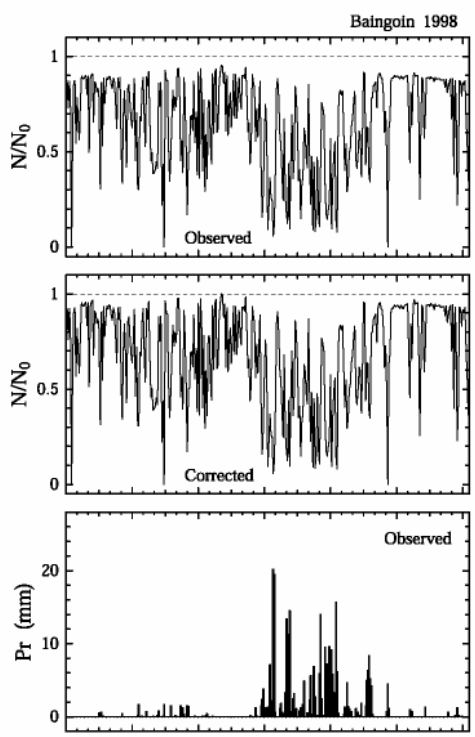

Fig.3

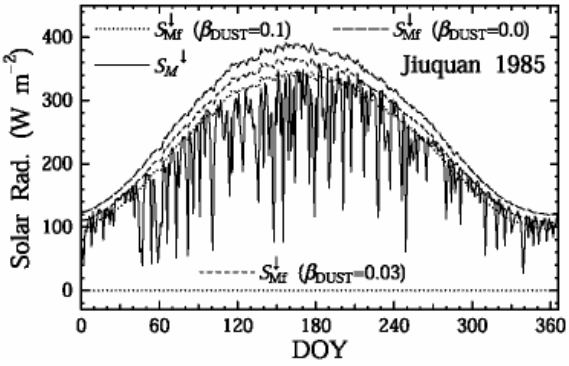

Fig.4

Fig. 5; The upper panel is the seasonal variation in solar radiation fluxes as observed by pyranometer and calculated from sunshine duration N for Lhasa in 1995. The solid line is the calculated SM↓ from N. The dotted line is SMf↓ under clear sky conditions with the Robinson's atmospheric turbidityβDUST = 0.02. Circles represent SM↓ observed by the pyranometer since 30 June 1995. The solar radiation ranges from about 100 Wm-2 to 380 Wm-2. Observed and calculated SM↓ agree. The lower panel shows the regression analysis of the observed and calculated SM↓. Regression analysis results suggest that the calculated values may be larger than observed values. Note, however, that data were observed only in the second half of the year.

Fig. 6; The left panel is the seasonal variation of the daily mean downward long-wave radiation flux LM↓ at Shiquanhe in 1998. Open circles are observed values and solid lines are calculated values. The right panel shows the regression analysis of the calculated and observed long-wave radiation. The calculations and observations agreevery well.

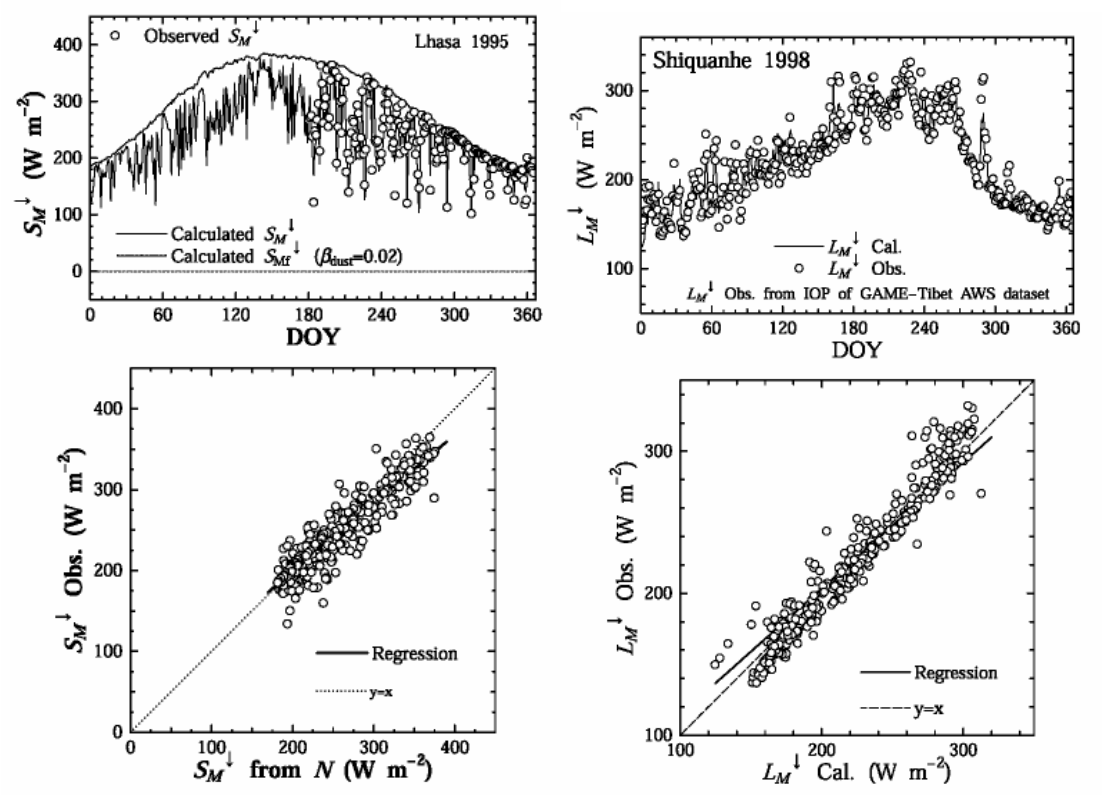

Fig. 5 **Fig.6**

3. Calculations and results

Calculations were performed for 31 stations in China. The calculation period was from 1971 to 2000. The Langley SRB dataset includes monthly means covering the period July 1983-June 1995 and was developed by the Radiation Sciences Branch of the Atmospheric Sciences Division at NASA, Langley Research Center, Hampton, Virginia. The irradiances are calculated using computationally fast radiative transfer algorithms whose primary input data are from the International Satellite Cloud Climatology Project (ISCCP) C1 products.

Fig. 7. Interannual variations in the surface radiation fluxes expressed by monthly mean values at Beijing from 1971-2000. The solid line is the monthly mean solar radiation SM↓, the dotted line is the long-wave radiation and the dashed line is the solar radiation from the Langley SRB dataset. The broken line and dotted chain are, respectively, SM↓and LM↓ trends obtained from line regression analysis. SM↓ changes from 83 Wm-2 (December) to 243 Wm-2 (February). The maximum and minimum monthly mean LM↓, 417 Wm-2 and 222 Wm-2, occur in July and January, respectively. Solar radiation has been decreasing at Beijing, perhaps as a result of increasing atmospheric

aerosols linked to its rapid development. Observed sunshine is also decreasing. Long-wave radiation has increased, and the rate of temperature change (Table 1) is large (0.0752 K yr-1).

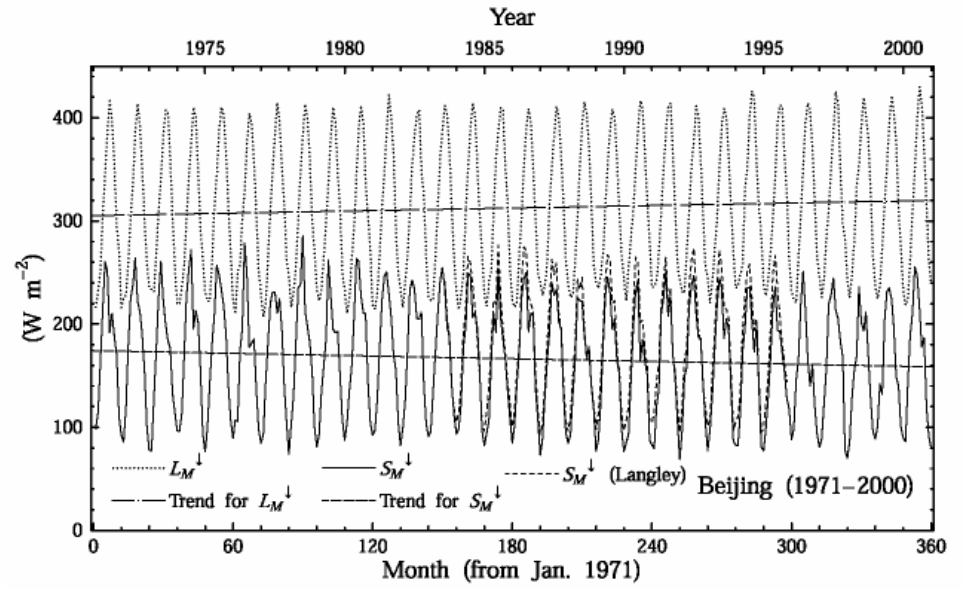

Fig. 7

Fig. 8. As in Fig.7, except for Hailar. Hailar (49.2°N, 119.8°E, 614m asl) is in rural northern China. SM↓and LM↓ are smaller than in Beijing. SM↓ changes from 47 Wm-2 (December) to 253 Wm-2 (June), LM↓ changes from 155 Wm-2 (January) to 360 Wm-2 (July). The mean values of SM↓ and LM↓ are 154 Wm-2 and 250 Wm-2, respectively (Table 1). SM↓ is decreasing and LM↓ is increasing.

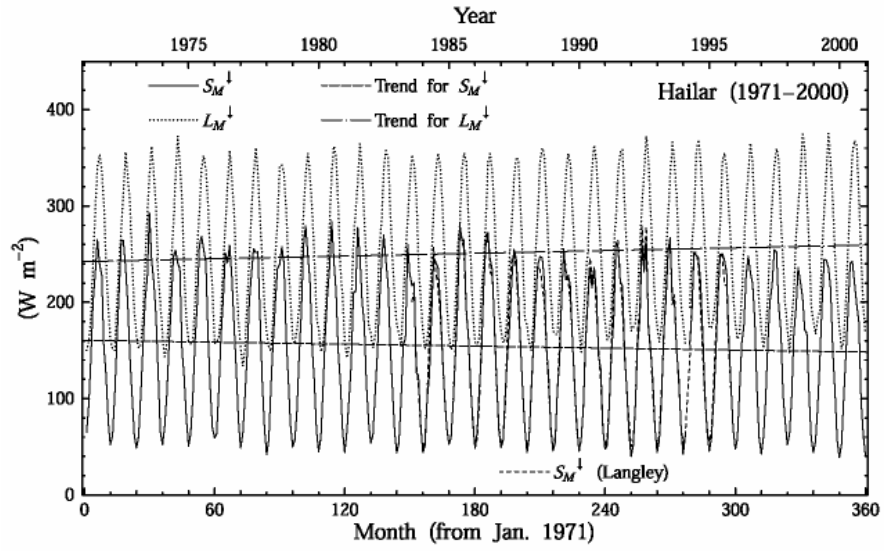

Fig.8

Fig. 9. As in Fig.7, except for Lhasa. Lhasa (29.7°N, 91.1°E, 3650m asl) is on the Tibetan Plateau. Variations in SM↓and LM↓ are very different from those at Beijing and Hailar. LM↓is larger than SM↓ at Beijing and Hailar, but they have similar values over Lhasa. As at Beijing and Hailar, SM↓is decreasing and LM↓ is increasing.

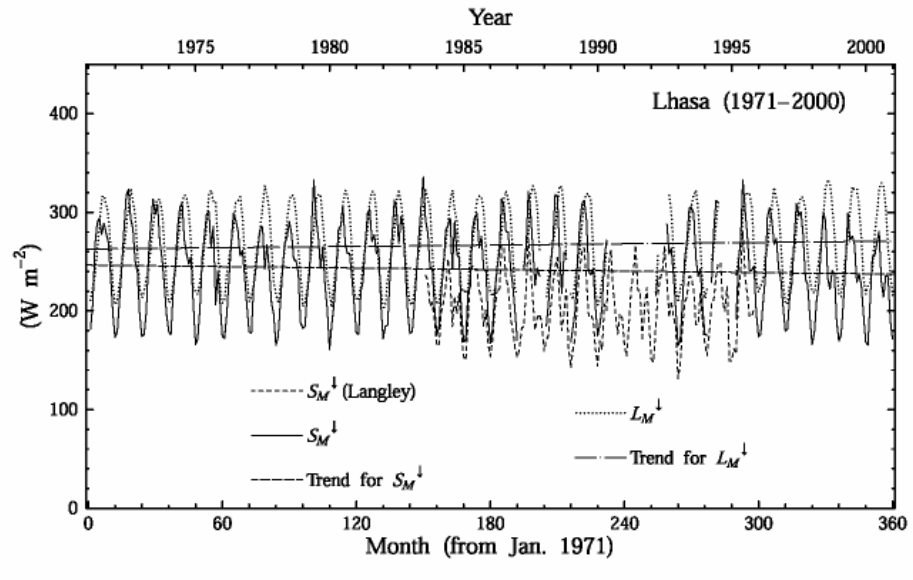

Fig.9

Fig. 10 The distribution of the solar radiation estimated from observed solar radiation duration for January, April, July, and October 1985.

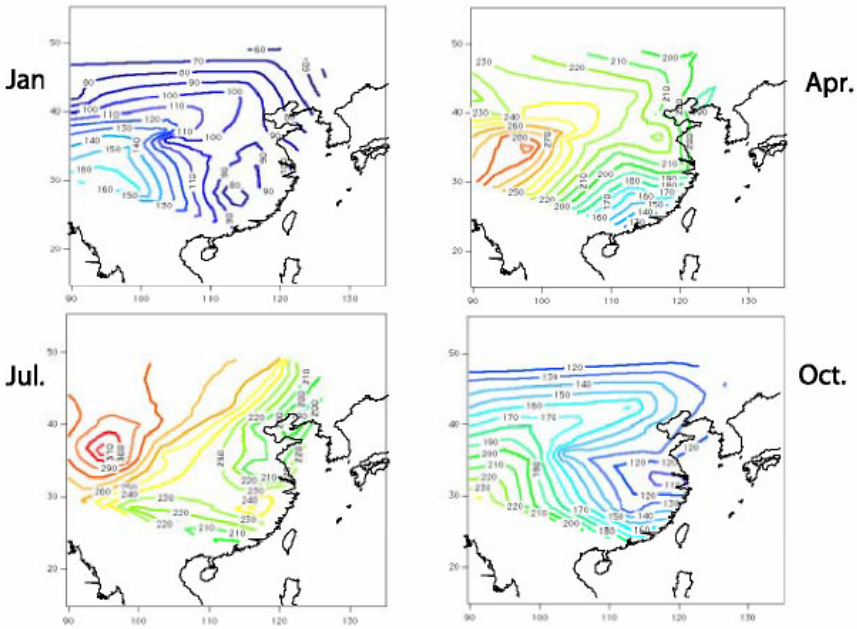

Fig.10

Table 1. Trends for each station from 1971-2000.

Name of the observatory	ΔT_A K yr^{-1}	Δe hPa yr^{-1}	ΔN hour yr^{-1}	$\Delta S_M^{\downarrow}$ Wm^{-2} yr^{-1}	$\Delta L_M^{\downarrow}$ Wm^{-2} yr^{-1}	$S_M^{\downarrow}$ Wm^{-2}	$L_M^{\downarrow}$ Wm^{-2}
Hailar	0.0777	0.02545	−11.692	−0.394	0.479	154.29	250.42
Bugt	0.0404	0.01313	6.893	0.216	0.076	154.75	248.37
Harbin	0.0648	0.02127	−12.971	−0.444	0.457	152.10	276.73
Altay	0.0461	0.02992	1.290	0.056	0.217	171.71	266.94
Fuyun	0.1024	0.00064	3.571	0.135	0.307	169.98	261.53
Urumqi	0.0220	−0.00152	−14.899	−0.474	0.259	168.47	282.33
Turpan	0.0641	−0.00941	−7.022	−0.220	0.323	172.01	315.24
Hotan	0.0359	0.01276	14.169	0.624	−0.030	184.78	302.76
Andir	0.0339	0.03613	−2.343	−0.113	0.261	190.51	289.11
Dunhuang	0.0372	0.00307	8.900	0.374	0.013	203.62	278.97
Jiuquan	0.0321	0.00606	5.639	0.248	0.067	198.18	272.48
Wushaoling	0.0387	0.00726	1.813	0.080	0.129	199.92	241.59
Golmud	0.0331	0.00253	3.633	0.165	0.072	223.00	251.98
Lanzhou	0.0659	−0.01633	−1.649	−0.047	0.250	183.00	294.91
Jurh	0.0524	−0.00135	−5.137	−0.208	0.273	194.86	260.38
Shenyang	0.0265	0.01047	−6.275	−0.273	0.202	155.02	297.60
Beijing	0.0752	−0.00576	−11.587	−0.484	0.436	166.42	312.52
Jinan	0.0358	0.02264	−16.855	−0.722	0.400	167.80	327.17
Lhasa	0.0384	0.00093	−7.313	−0.353	0.251	241.55	266.16
Madio	0.0372	0.00225	5.603	0.239	0.028	227.48	221.84
Deqen	0.0529	0.02371	−10.617	−0.480	0.406	196.93	274.31
Xi'an	0.0449	−0.01299	−25.995	−1.094	0.510	139.96	334.99
Lushi	0.0095	0.00414	6.512	0.276	−0.040	157.85	322.42
Changsha	0.0095	0.00342	−9.333	−0.437	0.188	136.47	355.89
Boxian	0.0332	0.00091	−14.941	−0.654	0.317	160.92	332.36
Dongtai	0.0334	0.00829	1.393	0.057	0.184	157.76	333.42
Hefei	0.0381	0.00213	−2.529	−0.110	0.213	148.49	342.90
Shanghai	0.0606	0.02051	−6.641	−0.300	0.417	148.33	344.56
Nanchang	0.0252	0.02585	−9.455	−0.436	0.278	149.85	354.02
Nanping	0.0285	0.01576	0.609	0.035	0.135	148.91	367.06
Guangzhou	0.0303	−0.00414	−14.647	−0.704	0.407	145.10	380.44

4. Summary and conclusion

(1) A method to estimate downward surface solar and long-wave radiation fluxes has been developed. The inputs are routine meteorological data. Fluxes were calculated at 31 stations in China using data from 1971 to 2000.

(2) Downward surface solar radiation flux was derived from sunshine duration data using parameters from a Jordan sunshine recorder. The surface long-wave radiation

flux was computed from the estimated solar radiation, the observed surface air humidity, and the temperature. Topographic influences and the effects of high altitude were considered. Calculations were verified by in situ observations.

(3) Over China, daily mean values of surface solar and long-wave radiation ranged from 140 - 240 Wm-2 and 220 - 380 Wm-2 , respectively. A map of the climatic distribution of surface solar radiation flux was presented.

(4) Climatic changes in the surface solar and long-wave radiation fluxes were investigated. The surface long-wave radiation flux at 29 out of 31 stations (Hotan and Lushi are the exceptions) has increased over the past 30 years. Surface solar radiation has decreased in large cities. Surface air temperature has increased at all 31 stations; vapor pressure has increased at most of the stations.

References

Kondo, J., and J. Xu, 1997: Seasonal variations in the heat and water balances for non-vegetated surfaces. J. Appl. Meteor., 36, 1676-1695.

Xu, J., and S. Haginoya, 2001: An estimation of heat and water balances in the Tibetan Plateau. J. Meteor. Soc. Japan, 71(1B),485-504.

Xu, J. 2001: An analysis of the climatic changes in the Eastern Asia using the potential evaporation, J. Japanese Soc. Hydro. And Water Resour., 14(2),151～170, (in Japanese with English summary)

Xu, J., S. Haginoya, K. Saito, and K. Motoya, 2003: Surface Heat and Water Balance Trends in Eastern Asia in the period 1971-2000. Hydrological Processes (in press)

Xu, J., S. Haginoya, K. Masuda, and R. Suzuki, 2004: An Estimation of heat and water balances over the Tibetan Plateau in 1997-1998. J. Meteor. Soc. Japan (in press)